Characterization of a Segmented n-Type Broad Energy Germanium Detector

Martin Schuster

Max-Planck Institute for Physics

July 21st, 2017

Physics Motivation: $0\nu\beta\beta$ Decay

Could provide information on:

- Nature of the neutrino: Dirac or Majorana?
- Inverted or Normal Hierarchy
- Possibly hints on absolute mass scale from $T_{1/2}$

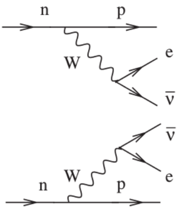

(a) $2\nu\beta\beta$

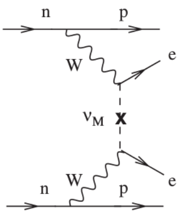

(b) $0\nu\beta\beta$

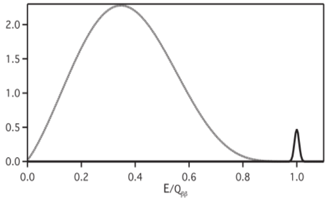

(c) Combined spectrum

Why Germanium?

- ^{76}Ge is a candidate for $0\nu\beta\beta$ and Ge is a semiconductor
- Can act as source and detector simultaneously
  $\rightarrow$ high detection efficiency
- Naturally good energy resolution
- Currently employed in experiments like GERDA and MAJORANA
- LEGEND collaboration is forming: Ton-scale germanium experiment

Point Contact Detector: Detection Principle

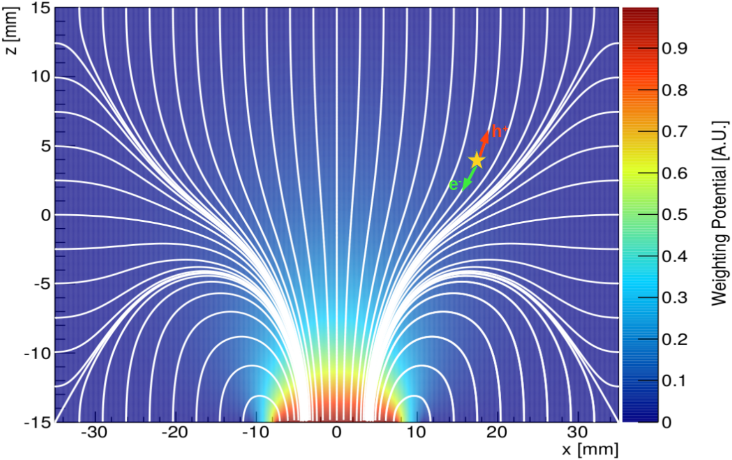

The Segmented Broad Energy Germanium Detector

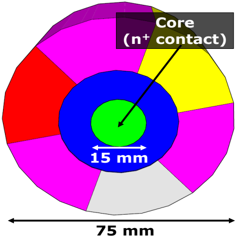

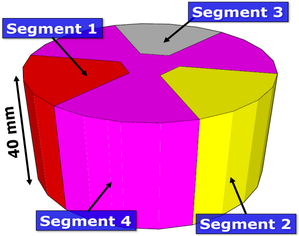

Features

- Point-Contact detector: Distinct Pulse Shapes
- Moderate Segmentation:
  - Information on ϕ location of energy depositions
  - Drifting Paths, Event Distributions, etc.

Example Pulse

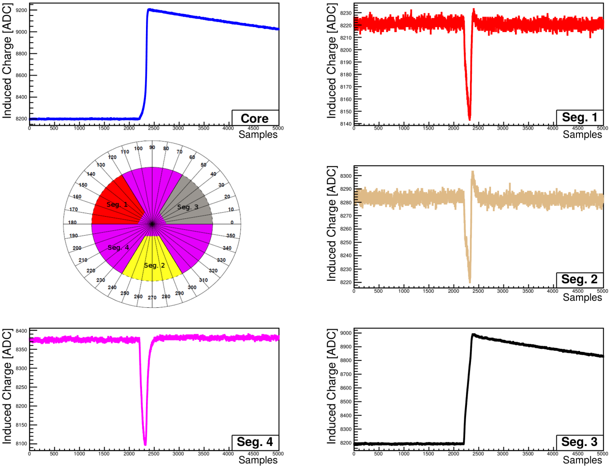

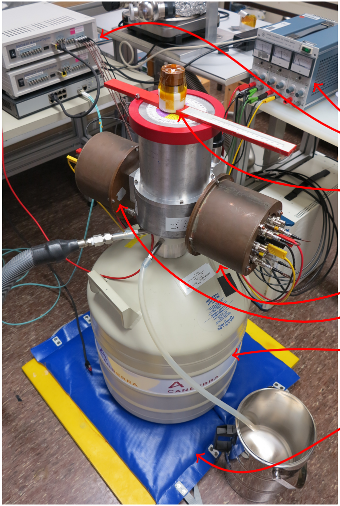

Experimental Setup

- DAQ and Preamplifier PSU
- Source with supporting structure on top of the cryostat
- Copper ears, containing the readout electronics
- LN_2 Dewar
- Foam mat and sand bags to reduce microphonic noise

Example Raw Core Pulse

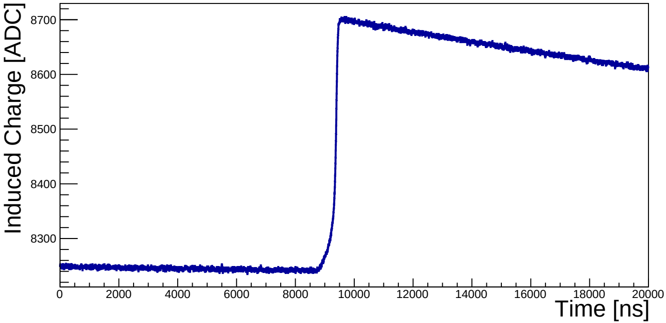

Fixed Window Method for Pulse Amplitude Determination

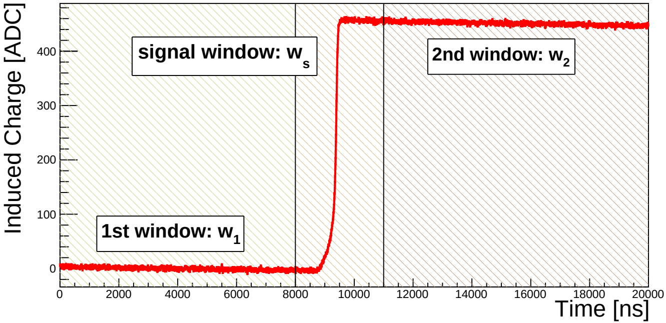

Crystal Axes Determination

- Slow and fast crystal axes influence the drift-path and speed of the charge carriers
- The dependence of t_{5-95} on ϕ is expected to be sinusoidal:

$$t_{5-95} = C + a \cdot \sin\left[\frac{2\pi}{90}\left(\phi + \phi_{offset}\right)\right] \quad .$$

The parameters C, a and ϕ_{offset} were fitted to the data

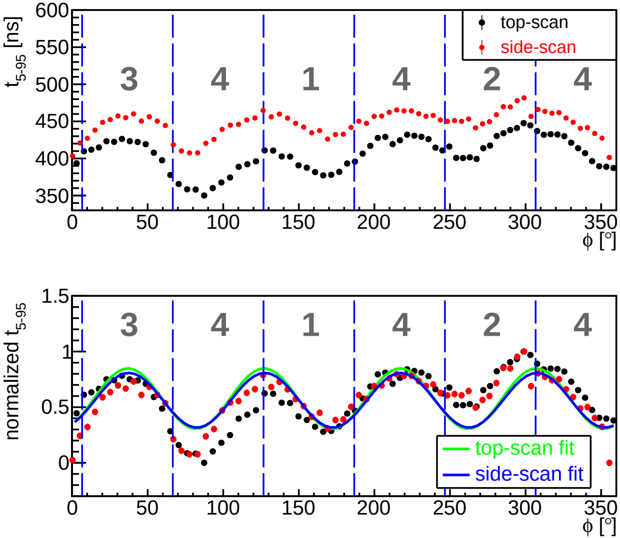

600
550
500
450
400
350
$t_{5\text{-}95}$ [ns]
top-scan
side-scan
3
4
1
4
2
4
0
50
100
150
200
250
300
350
ϕ [°]
1.5
1
0.5
0
normalized $t_{5\text{-}95}$
top-scan fit
side-scan fit

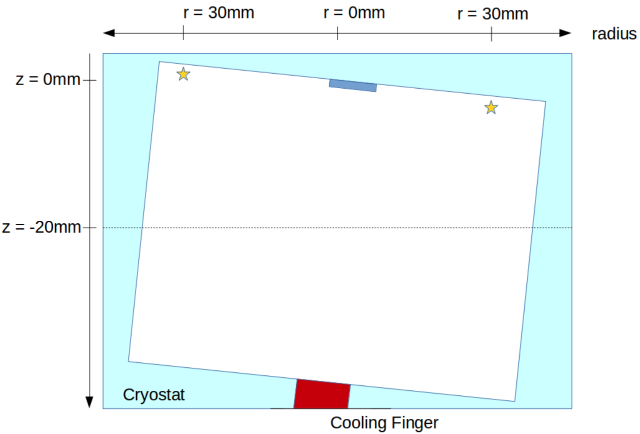
r = 30mm
r = 0mm
r = 30mm
radius
z = 0mm
z = -20mm
Cryostat
Cooling Finger

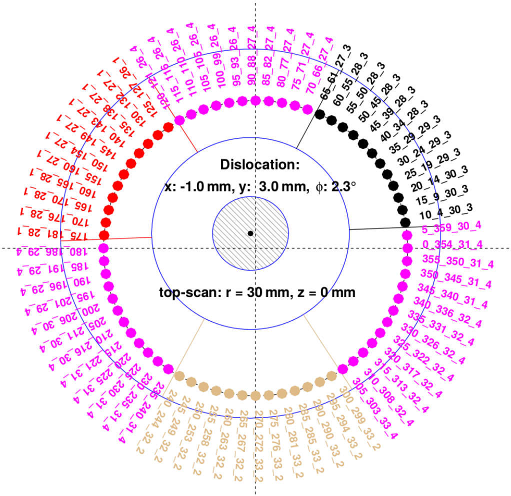
Dislocation:
x: -1.0 mm, y: 3.0 mm, ϕ: 2.3°
top-scan: r = 30 mm, z = 0 mm

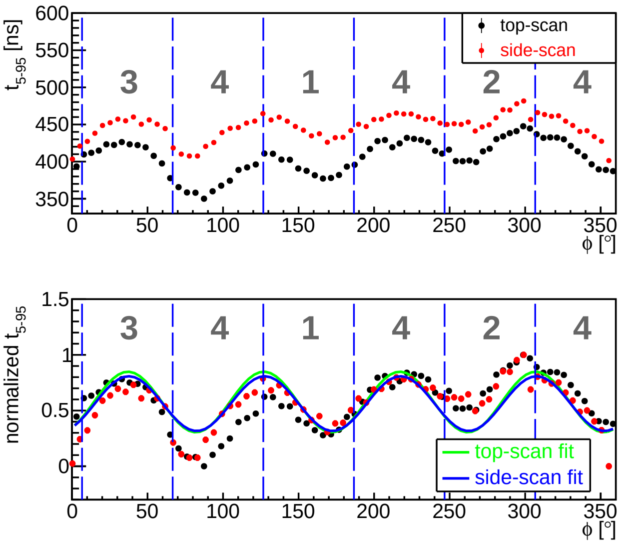

t_{5-95} [ns]
600
550
500
450
400
350
0
50
100
150
200
250
300
350
ϕ [°]
3
4
1
4
2
4
top-scan
side-scan
normalized t_{5-95}
1.5
1
0.5
0
top-scan fit
side-scan fit

Localizing ϕ *Position* using Mirror Pulses

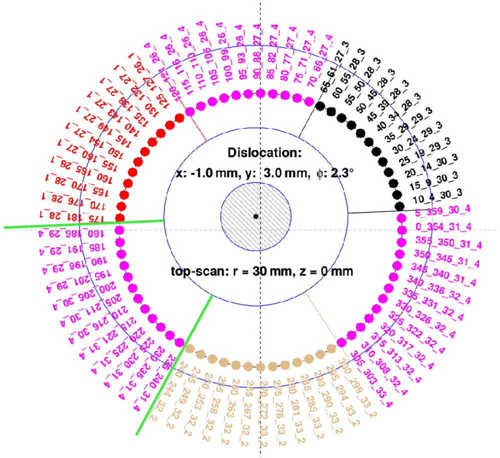

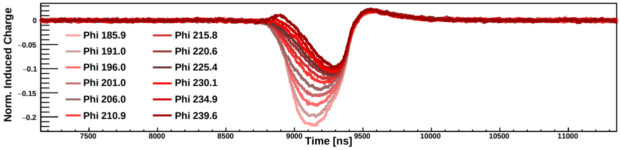
Norm. Induced Charge
0
−0.05
−0.1
−0.15
−0.2
Phi 185.9
Phi 191.0
Phi 196.0
Phi 201.0
Phi 206.0
Phi 210.9
Phi 215.8
Phi 220.6
Phi 225.4
Phi 230.1
Phi 234.9
Phi 239.6
7500
8000
8500
9000
9500
10000
10500
11000
Time [ns]

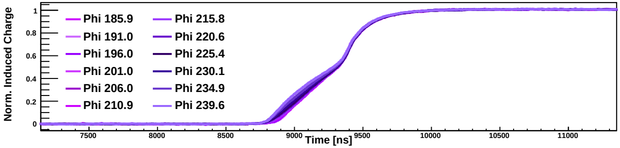
Norm. Induced Charge
1
0.8
0.6
0.4
0.2
0
Phi 185.9
Phi 191.0
Phi 196.0
Phi 201.0
Phi 206.0
Phi 210.9
Phi 215.8
Phi 220.6
Phi 225.4
Phi 230.1
Phi 234.9
Phi 239.6
7500
8000
8500
9000
9500
10000
10500
11000
Time [ns]

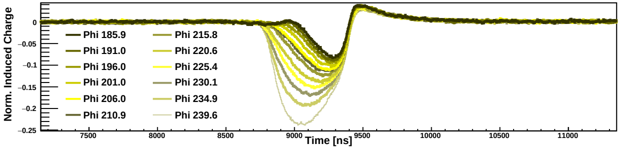
Norm. Induced Charge
0
−0.05
−0.1
−0.15
−0.2
−0.25
Phi 185.9
Phi 191.0
Phi 196.0
Phi 201.0
Phi 206.0
Phi 210.9
Phi 215.8
Phi 220.6
Phi 225.4
Phi 230.1
Phi 234.9
Phi 239.6
7500
8000
8500
9000
9500
10000
10500
11000
Time [ns]

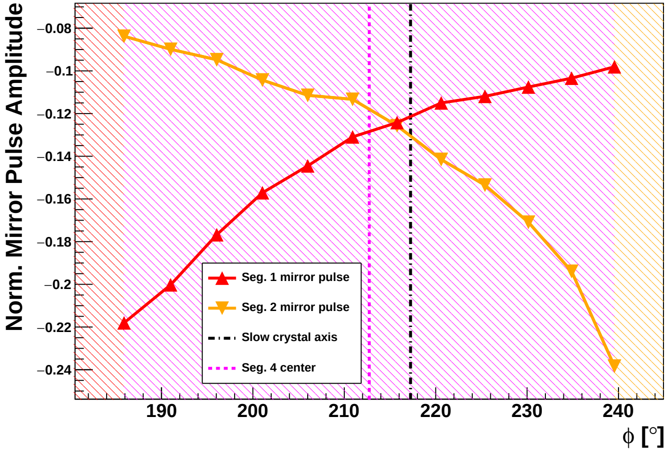
Norm. Mirror Pulse Amplitude
−0.08
−0.1
−0.12
−0.14
−0.16
−0.18
−0.2
−0.22
−0.24
190
200
210
220
230
240
ϕ [°]
Seg. 1 mirror pulse
Seg. 2 mirror pulse
Slow crystal axis
Seg. 4 center

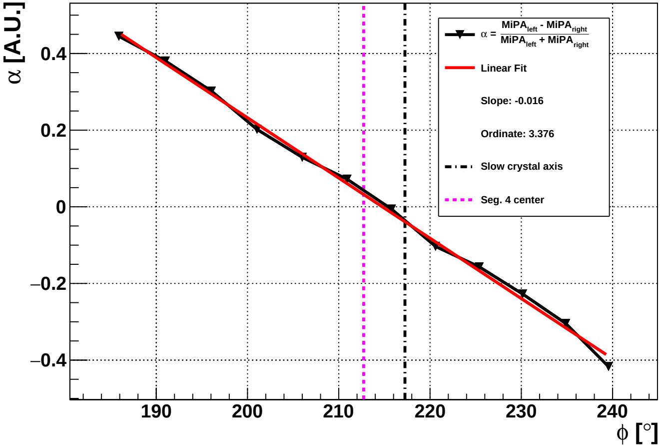
α [A.U.]
0.4
0.2
0
−0.2
−0.4
190
200
210
220
230
240
ϕ [°]
$\alpha = \frac{MiPA_{left} - MiPA_{right}}{MiPA_{left} + MiPA_{right}}$
Linear Fit
Slope: -0.016
Ordinate: 3.376
Slow crystal axis
Seg. 4 center

Passivation Layer Studies

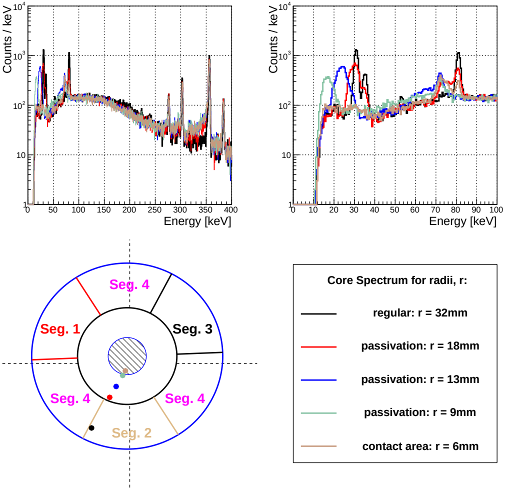

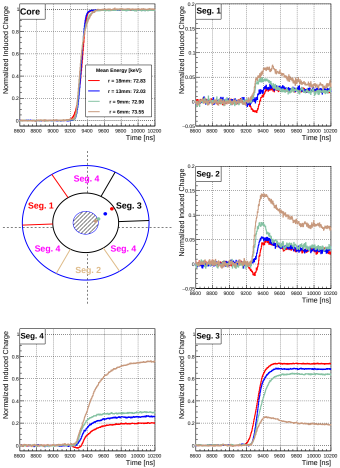

- Both segment 3 and 4 are collecting
- Truncated mirror pulses: Indication for charge trapping
- Increasing effect for smaller radii

Near Surface Effects: Distorted Field Lines

- Drift paths are bent towards the surface, where the electric field is very weak
- At surface, the charge-drift slows down significantly
- This gives rise to the obeserved phenomena via two mechanics:
  - Incomplete charge collection: Charges cease to contribute to the pulse
  - Strongly delayed pulses: Pulses don't reach their amplitude during DAQ-window

Summary and Results

- Prototype detector, combining the point contact layout with a moderate segmentation.
- Localization of the crystal axes, despite tilted installation: Good agreement between top-scans and side-scans
- Reconstructing the ϕ-position using mirror pulses of non-collecting segments: Proven to be feasible
- Indication of distorted drift paths for low energy events beneath the passivated area
  The effects show a significant r dependence, yet they are independent on ϕ

Outlook

- The detector has been moved to new, electrically cooled cryostat
- Measurements of temperature dependence of passivation layer effects and drift times in general
- Expanding and refining the event position reconstruction, including Monte-Carlo based pulse-shape libraries
- Further studies on the effect of the crystal axes (also temp. dep.)

Glorious Times Ahead...

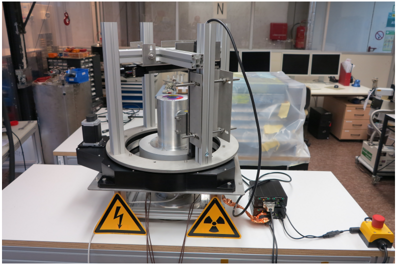

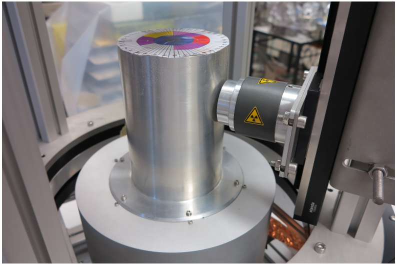

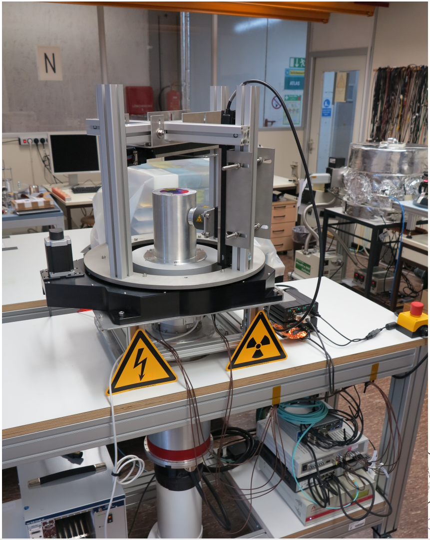

Thank you for your attention!

BACKUP

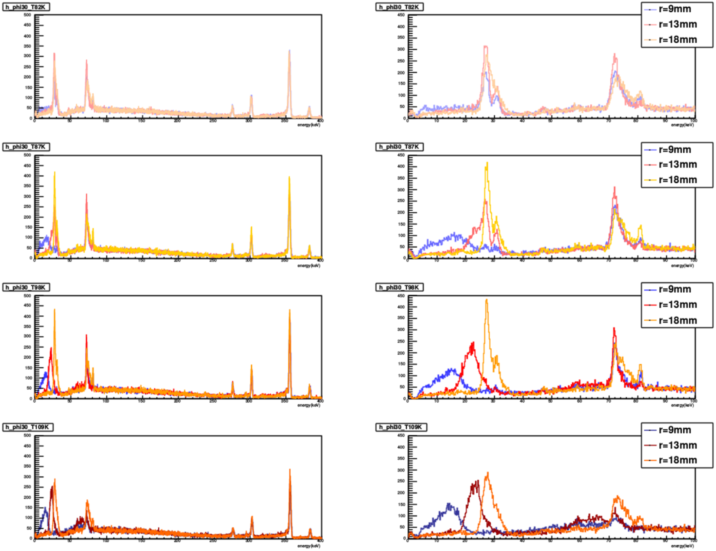
h_phi30_T82K
h_phi30_T82K
r=9mm
r=13mm
r=18mm
h_phi30_T87K
h_phi30_T87K
r=9mm
r=13mm
r=18mm
h_phi30_T98K
h_phi30_T98K
r=9mm
r=13mm
r=18mm
h_phi30_T109K
h_phi30_T109K
r=9mm
r=13mm
r=18mm
energy(keV)

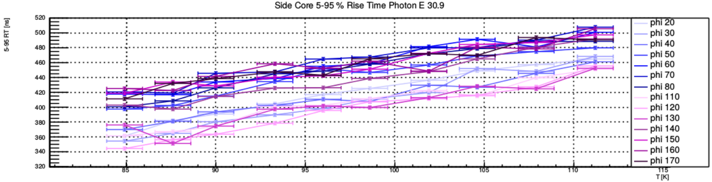
Side Core 5-95 % Rise Time Photon E 30.9
5-95 RT [ns]
T [K]
phi 20
phi 30
phi 40
phi 50
phi 60
phi 70
phi 80
phi 110
phi 120
phi 130
phi 140
phi 150
phi 160
phi 170

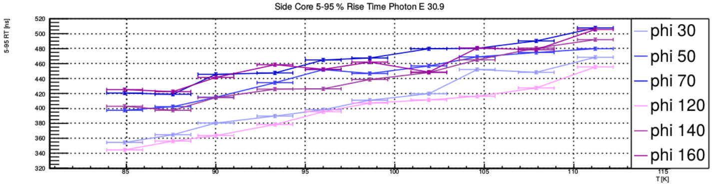
Side Core 5-95 % Rise Time Photon E 30.9
5-95 RT [ns]
T [K]
phi 30
phi 50
phi 70
phi 120
phi 140
phi 160

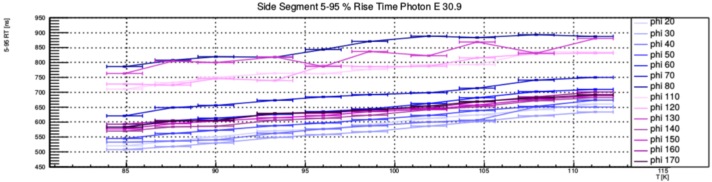
Side Segment 5-95 % Rise Time Photon E 30.9
5-95 RT [ns]
T [K]
phi 20
phi 30
phi 40
phi 50
phi 60
phi 70
phi 80
phi 110
phi 120
phi 130
phi 140
phi 150
phi 160
phi 170

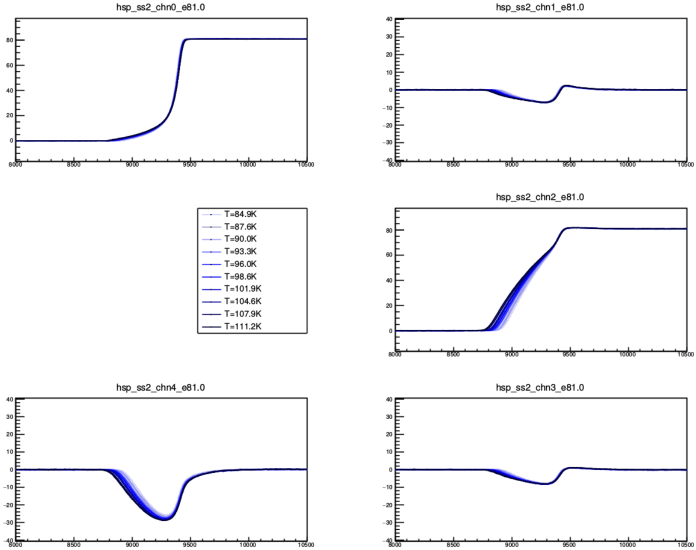

Figure 69: The super pulses of 81 keV at $\phi = 30°$ (segment 2) with the source on the side

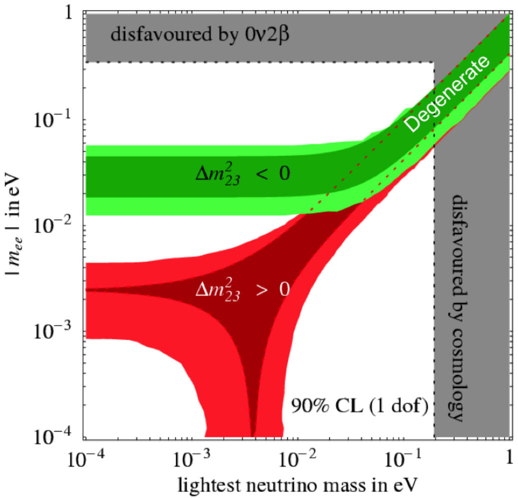

1

[1] I. Gil-Botella, Neutrino Physics (2015)

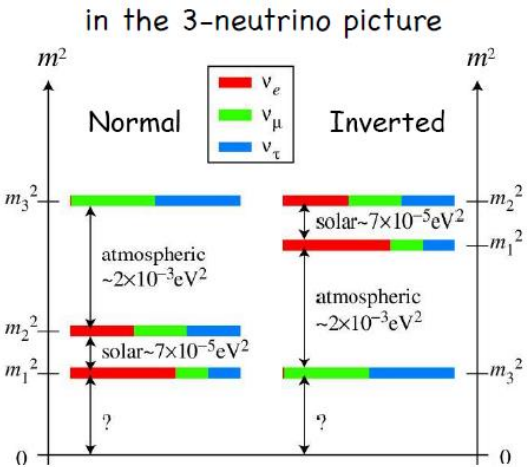
in the 3-neutrino picture
m²
m²
νe
νμ
ντ
Normal
Inverted
m₃²
m₂²
m₁²
m₂²
m₁²
m₃²
atmospheric
~2×10⁻³eV²
solar~7×10⁻⁵eV²
solar~7×10⁻⁵eV²
atmospheric
~2×10⁻³eV²
?
?
0
0

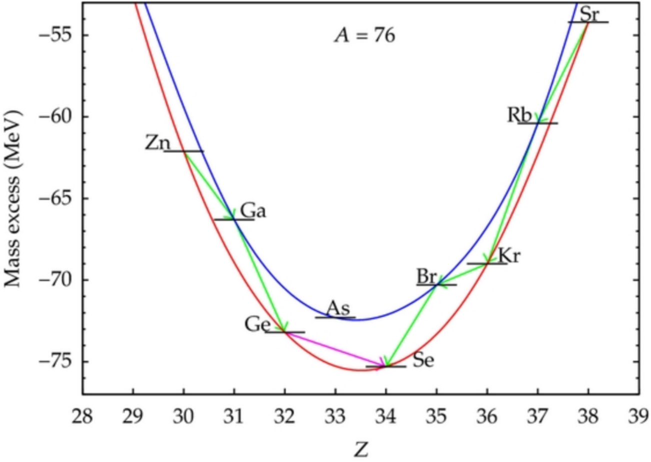

2

[2] A. Giullani and A. Poves, Advances in High Energy Physics(2012)

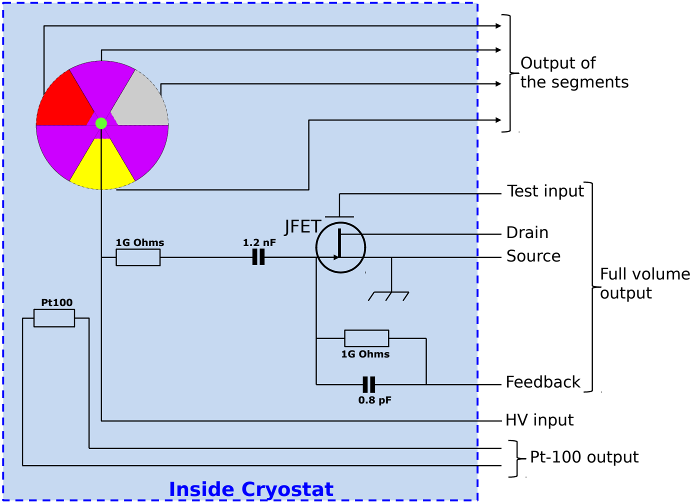
Output of
the segments
Test input
JFET
Drain
Source
1G Ohms
1.2 nF
Full volume
output
Pt100
1G Ohms
Feedback
0.8 pF
HV input
Pt-100 output
Inside Cryostat

Multi-Site- vs. Single-Site-Event Discrimination

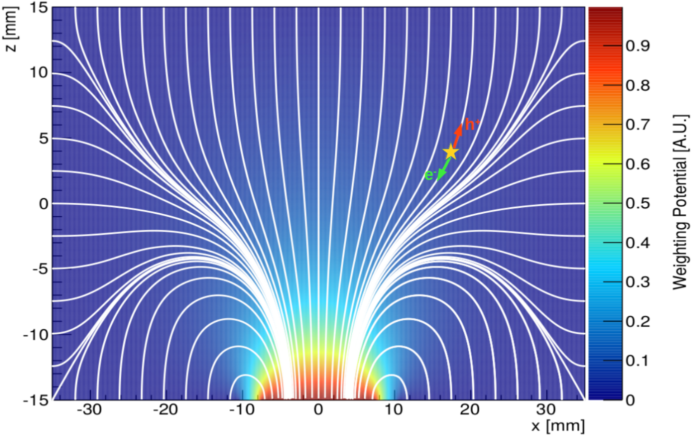

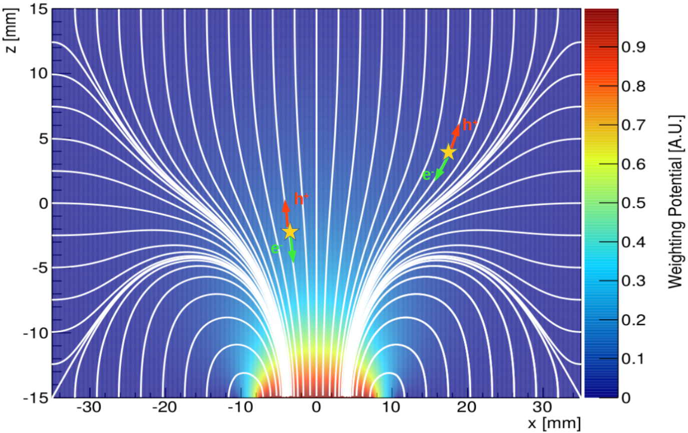

z [mm]
15
10
5
0
-5
-10
-15
-30
-20
-10
0
10
20
30
x [mm]
h+
e-
h+
e-
0.9
0.8
0.7
0.6
0.5
0.4
0.3
0.2
0.1
0
Weighting Potential [A.U.]

A/E Method

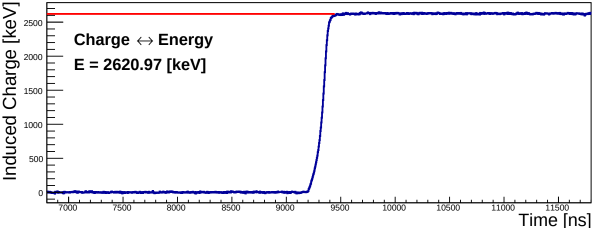
Induced Charge [keV]
Charge ↔ Energy
E = 2620.97 [keV]
Time [ns]
0
500
1000
1500
2000
2500
7000
7500
8000
8500
9000
9500
10000
10500
11000
11500

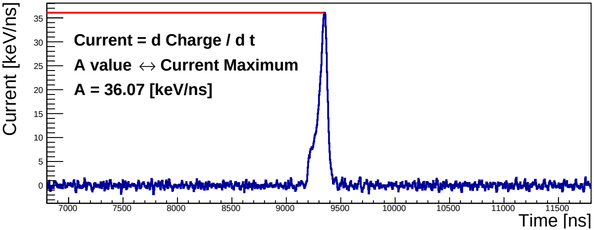
Current [keV/ns]
Current = d Charge / d t
A value ↔ Current Maximum
A = 36.07 [keV/ns]
Time [ns]
0
5
10
15
20
25
30
35
7000
7500
8000
8500
9000
9500
10000
10500
11000
11500

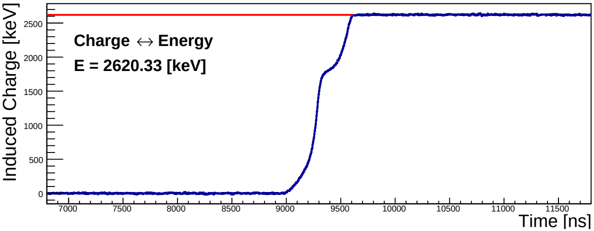
Charge ↔ Energy
E = 2620.33 [keV]
Induced Charge [keV]
0
500
1000
1500
2000
2500
7000
7500
8000
8500
9000
9500
10000
10500
11000
11500
Time [ns]

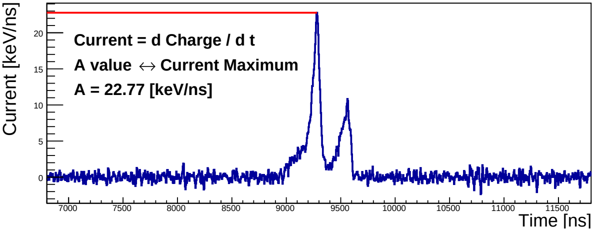
Current = d Charge / d t
A value ↔ Current Maximum
A = 22.77 [keV/ns]
Current [keV/ns]
0
5
10
15
20
7000
7500
8000
8500
9000
9500
10000
10500
11000
11500
Time [ns]

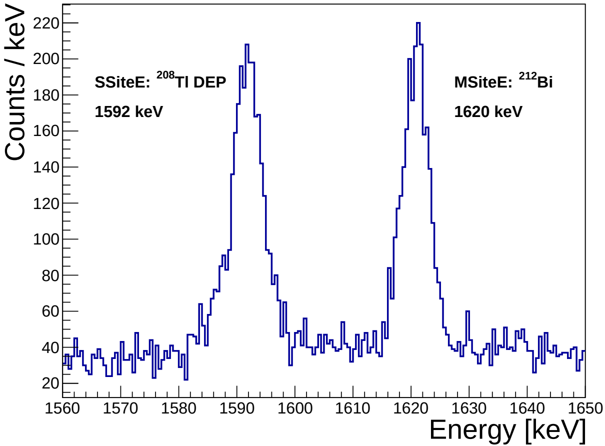

SSiteE: 208Tl DEP
1592 keV
MSiteE: 212Bi
1620 keV
Counts / keV
220
200
180
160
140
120
100
80
60
40
20
1560
1570
1580
1590
1600
1610
1620
1630
1640
1650
Energy [keV]

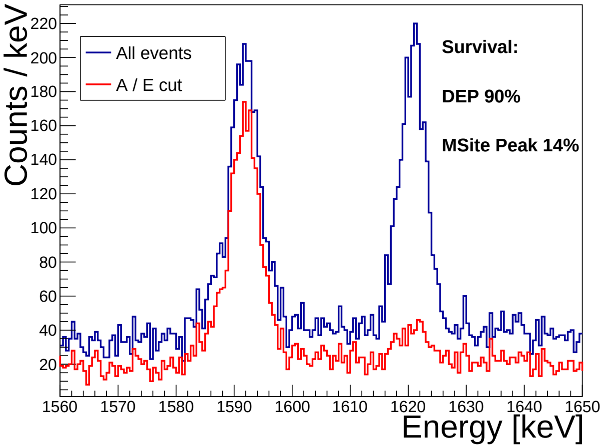
Counts / keV
All events
A / E cut
Survival:
DEP 90%
MSite Peak 14%
Energy [keV]
220
200
180
160
140
120
100
80
60
40
20
1560
1570
1580
1590
1600
1610
1620
1630
1640
1650

Segmentation Cut

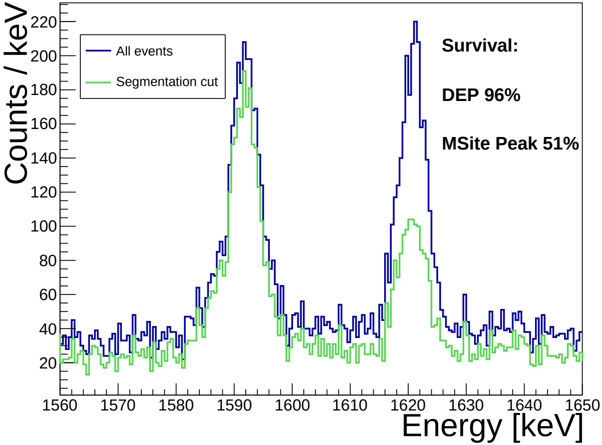

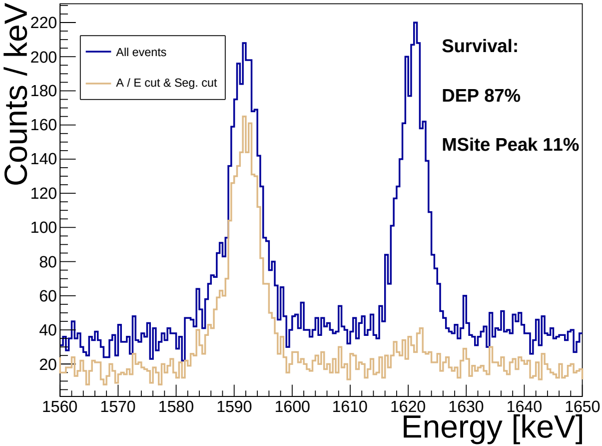
All events
A / E cut & Seg. cut
Survival:
DEP 87%
MSite Peak 11%
Counts / keV
Energy [keV]
20
40
60
80
100
120
140
160
180
200
220
1560
1570
1580
1590
1600
1610
1620
1630
1640
1650

After the cross-talk correction and energy calibration procedure, Tab 1 gives an overview of the energy resolutions for selected γ-lines and all the segments.

		FWHM [keV]				
Source	**γ-line [keV]**	**Core**	**Seg. 1**	**Seg. 2**	**Seg. 3**	**Seg. 4**
^{133}Ba	81	3.29	5.15	4.05	4.07	7.26
	356	2.64	4.58	3.47	3.52	6.04
^{60}Co	1173	4.57	4.88	4.16	4.34	8.05
	1332	4.93	5.00	4.39	4.14	7.84
^{228}Th	2614	7.65				

Table: Energy resolutions as absolute FWHM in keV. The resolutions for especially characteristic γ-lines for the respective sources are given.

Segment	Boundary(i, j)	Top-scan	Side-scan
1	$\phi_{4,1}$	124.7 ± 0.6	120.0 ± 0.8
	$\phi_{1,4}$	181.1 ± 0.6	181.1 ± 0.8
2	$\phi_{4,2}$	244.0 ± 0.6	242.5 ± 0.7
	$\phi_{2,4}$	302.5 ± 0.6	302.1 ± 0.8
3	$\phi_{4,3}$	7.1 ± 0.5	3.8 ± 0.7
	$\phi_{3,4}$	64.8 ± 0.6	63.5 ± 0.7
4	$\phi_{3,4}$	66.6 ± 0.6	62.8 ± 0.7
	$\phi_{4,1}$	123.0 ± 0.6	120.2 ± 0.8
	$\phi_{1,4}$	182.5 ± 0.5	180.8 ± 0.7
	$\phi_{4,2}$	242.4 ± 0.6	242.3 ± 0.6
	$\phi_{2,4}$	303.2 ± 0.8	302.0 ± 0.7
	$\phi_{4,3}$	6.2 ± 0.5	3.4 ± 0.6

Scan	ϕ_{offset}	$\phi_{\langle 110 \rangle}$
Top	-14.52 $\pm$ 0.24	37.02 $\pm$ 0.24
Side	-15.05 $\pm$ 0.30	37.55 $\pm$ 0.30

Table: The values of ϕ_{offset} and $\phi_{\langle 110 \rangle}$, see Eq. 14, as determined by fits to the data.

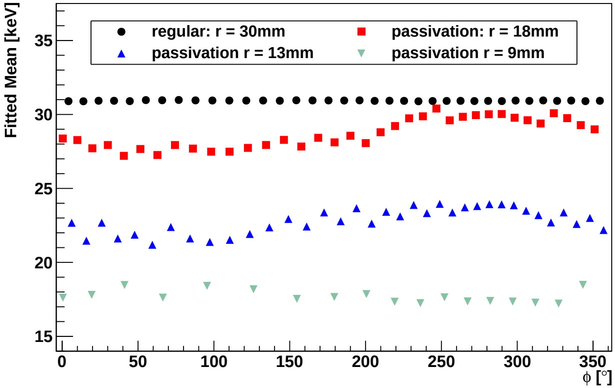
regular: r = 30mm
passivation: r = 18mm
passivation r = 13mm
passivation r = 9mm
Fitted Mean [keV]
15
20
25
30
35
0
50
100
150
200
250
300
350
ϕ [°]

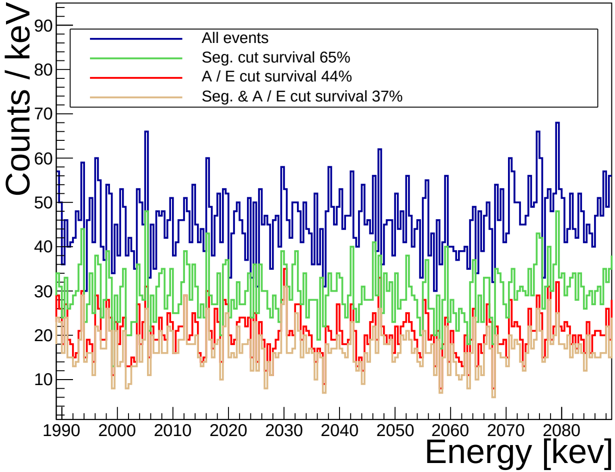
Counts / keV
90
80
70
60
50
40
30
20
10
All events
Seg. cut survival 65%
A / E cut survival 44%
Seg. & A / E cut survival 37%
1990
2000
2010
2020
2030
2040
2050
2060
2070
2080
Energy [kev]